Fracture strength and fatigue endurance in Gd-doped ceria thermal actuators

Fracture Strength and Fatigue Endurance in Gd-Doped Ceria Thermal Actuators

Eran Mishuk[1], Andrei Ushakov[2], Jenny Shklovsky[3], Slava Krylov[5], Yosi Shacham-Diamand[3], Vladimir Ya. Shur[2], Andrei Kholkin[4], and Igor Lubomirsky[1]

1 Department of Materials and Interfaces, Weizmann Institute of Science, Herzl St 234, Rehovot 7610001, Israel.
2 School of Natural Sciences and Mathematics, Ural Federal University, Lenin Ave. 51, Ekaterinburg 620000, Russia.
3 Department of Physical Electronics, School of Electrical Engineering, Tel Aviv University, Israel 69978
4 CICECO-Aveiro Institute of Materials, Department of Physics and, University of Aveiro, 3810-193 Aveiro, Portugal.
5 School of Mechanical Engineering, Tel Aviv University, Israel 69978

Abstract

We studied the stability of the mechanical properties and the fatigue endurance of Gd-doped ceria (CGO), which is a promising electromechanically active material for microelectromechanical systems (MEMS). Specifically, the fracture strength and long-term operation of plate-type circular (2 mm diameter) thermal actuators made of ≈1.15 μm thick $Ce_{0.95}Gd_{0.05}O_{1.975}$ (CGO5) were investigated. Excitation voltage of 10 V at the frequency range between 1 and 2.1 MHz induces Joule heating effect that can generate an in-plane strain of ≈0.1%. The operation temperature ranged from 25°C to 80°C and the temperature shift, caused by the AC heating, was about 80K at 10V. Critical fracture was found to occur at out-of-plane displacements between ~35 and ~42 μm, which corresponds to the average bending stress of ~44 MPa at the center of the plate. During long-term operation, the actuators exhibit gradual decrease in the response, probably due to contact degradation. However, structural damage or mechanical fatigue was not found even after 10^7 cycles at a stress level of ~30% of the critical fracture strength.

Keywords: MEMS, Actuator, Doped ceria, Fatigue

1 Introduction

Integration of functional ceramic materials (e.g. piezoelectric and electrostrictive materials) into microelectromechanical systems (MEMS) is one of the promising strategies for miniaturization of sensors and actuators.[1] The widely used piezoelectric ceramics, Lead Zirconate-Titanate ($PbZr_{1-X}Ti_xO_3$ or PZT), contains lead, which is known to be one of the most toxic environmental and industrial pollutants; Therefore, the use of lead and its compounds is prohibited by most fabrication facilities.[2] An intensive research has been carried out exploring lead free materials with suitable characteristics that can be integrated with micro and nano fabricated devices.

Gadolinium-doped ceria, $Ce_xGd_{1-x}O_{2-x/2}$ (CGO), an extensively studied ion-conductor, [3, 4] is the first low dielectric/low mechanical-compliance material that exhibits large electrostriction effect exceeding 10^{-17} m^2/V^2. [5-10] The electrostrictive properties of CGO have been previously studied in bulk ceramics and thin films. [8, 10, 11] The feasibility of incorporating CGO as electromechanically active material in MEMS actuators has been recently demonstrated for circular self-supported membranes. [9, 12] While the phenomenological aspect of the electrostriction effect has been studied quite extensively, very little is known about the stability of mechanical and electrical properties of CGO-based MEMS devices.

This work focuses on study of the fracture strength and long-term material properties stability of thermal actuators based on $Ce_{0.95}Gd_{0.05}O_{1.975}$ (CGO5) films. Here we show that circular 2 mm diameter self-supported Al/Ag/Ti/CGO5/Ti/Al plates can withstand forty million cycles of 0.03 % strain without mechanical failure. CGO5 was chosen since it exhibits electrostriction response larger than CGO films with higher Gd content. [13] Nevertheless, the results of this study are not expected to be substantially different for membranes made of CGO films with higher Gd content.

2 Experimental details

2.1 Device fabrication

Self-supported membranes of an Al/Ag/Ti/CGO5/Ti/Al layered structure (Figure 1a) were prepared by silicon bulk micromachining, similar to a procedure reported earlier.[9] Note that, despite that the device has certain bending stiffness, for the sake of consistency, we mainly refer it hereafter as "membrane" rather than "plate". The membranes consist of 1.15 μm thick CGO5 layers confined between 340 nm thick bottom Al/Ag/Ti contact (Figure 1b) and 200 nm thick top Ti/Al contact. In brief, the preparation procedure is as follows: Al and Ag layers (180 nm and 100 nm thick, respectively) were sequentially deposited with an electron-beam evaporator (ODEM Selen 500 evaporation system) on a Si substrate (275 μm thick, undoped). The Ti and the CGO5 films were deposited by DC and RF magnetron sputtering (ATC Orion Series Sputtering System, AJA International Inc.). The films were annealed at 450 °C for 5 hours in a tube oven under N_2 (99.999%) flow and cooled down to room temperature at a rate of 1K/min. Electron-beam evaporation was then used to deposit Ti and Al (each 100 nm thick) layers on the CGO for contact and a backside Al (300 nm thick) layer was deposited on the Si for mask. The Top Ti/Al contacts and the backside. Al layers were patterned by photolithography and etched with an HF (5% v/v) solution. The self-supported membranes were obtained by etching through the entire thickness of the Si substrate using a dry reactive ion etch (DRIE). In this process, the bottom Al film served as an etch-stopping layer. The Al/Ag film enabled stress relaxation during annealing. The Ti layer provides an Ohmic contact and a good adhesion to the CGO layer.[9]

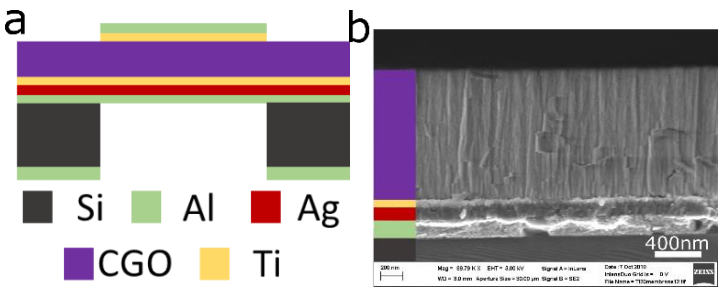

Figure 1. (a) Schematic of the device showing the layered structure. (b) SEM image of a device cross-section.

The circular 2 mm diameter membranes displayed a perfectly flat shape at room temperature (**Figure 2**a). The membranes buckle upon heating due to the thermal expansion (Figure 2b and Figure 2c). The buckling temperature was between 45 and 65°C, depending on the sample. Upon cooling back to room temperature, the plates restore the original flat shape.

Comparison of the thermal strains corresponding to the measured buckling temperatures with the critical buckling values for the circular, thin, fully clamped, stress-free plate [14] indicated that our structures were under tensile stress in the initial, as-fabricated, state. To illustrate this point, the effective thermal expansion coefficient (TEC) of the stack of materials that the membrane was first estimated. Using optical profilometry (Figure 2d) the shape of the plate in the post-buckled state was monitored at the temperatures between the buckling value and 140°C. The thermally induced actual in-plane strain was estimated from the increase of the buckled plate diameter arc length according to the expression

(1) $$u_{th} = \frac{L_{Tf} - L_{Ti}}{L_{Ti}},$$

where L_{Tf} and L_{Ti} are the lengths of the profile at the final and initial temperatures, respectively. For the membrane shown in Figure 2, buckling starts at 45 °C and the thermally induced strain increases linearly with temperature (Figure 2e) with the slope of TEC =10.4 ± 0.4×10^{-6} K^{-1}, which is close to the earlier reported values.[14] With the value of TEC in hand, one can deduce that for the membrane shown in Figure 2, the actual measured buckling strain is u_{crit}= TEC × (45°C -25°C) = 2.1 ± 0.1×10^{-4}. This strain includes two contributions: the residual in-plane strain of the plate and the compressive thermal in-plane strain. The theoretical critical buckling strain for a thin plate with the thickness of $1.7\ \mu m$ and the diameter of 2 mm is u_{theor}=3.5×10^{-6} [15, 16], which is two orders of magnitude smaller than the measured u_{crit}. One may conclude therefore that at room temperature our membranes withstand ≈2×10^{-4} tensile strain without disintegration. The buckling occurs when the difference between the thermally induced compressive stress and the tensile residual stress exceeds the critical buckling value. Since the tensile residual stress is much larger than the critical buckling stress, prior the buckling the plate essentially behaves as a membrane, it is to say, as a structure with its effective stiffness dominated by the in-

plane tension rather than by the bending stiffness. However, the shape of the structure in the post-buckled state is dictated by its bending stiffness, especially near the clamped boundary.

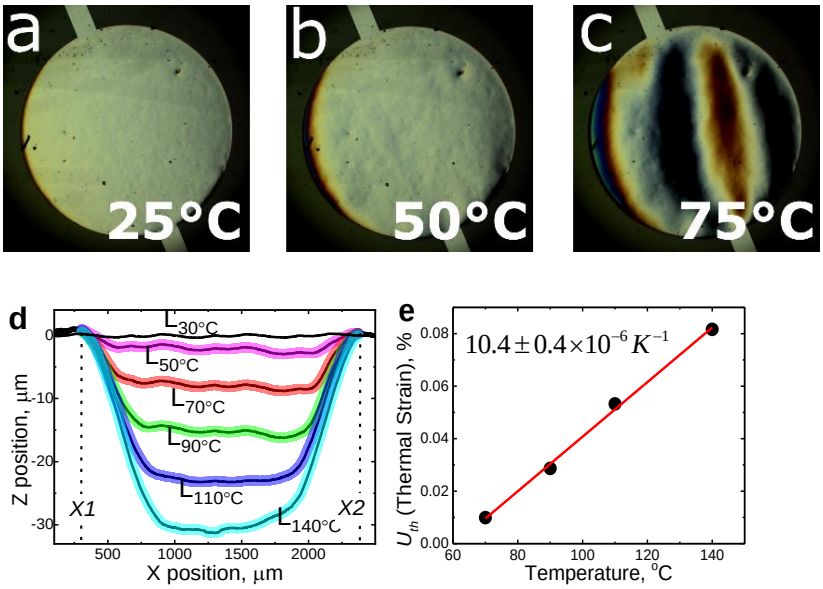

Figure 2. Optical microscope image (using circular differential interference contrast, C-DIC, Axio, Zeiss) of a self-supported Al/Ag/Ti/CGO5/Ti/Al plate at (a) 25˚C, (b) 50˚C and (c) 75˚C. (d) Line-profile, measured with an optical profiler (ZETA-20), at the center of a buckled plate at different temperatures between 50˚C and 140˚C. The lengths of the profiles at the different temperatures were measured between points *X1* and *X2* labeled in the panel. (e) Thermally induced strain of the profiles measured in (d) as a function of temperature. The thermal strain was calculated with respect to the profile at 50˚C as the initial state using Eq. (1). The linear fit (red line) corresponds to thermal expansion coefficient labeled in the panel.

2.2 Measurement of electro-thermal actuation

As reported earlier, the electrostrictive response of CGO is large (>$10^{-17} m^2/V^2$) only below 1 Hz.[7, 9, 10] Therefore, a test, comprising several thousand actuation cycles via the electrostriction effect, would be very time consuming. To circumvent this problem, for the current study, we used electro-thermal actuation by applying the high frequency (within the range between 1 MHz and up to 2.1 MHz) excitation voltage modulated by a few Hz-envelope. At 2.1 MHz, the impedance of the film is close to that at 50 Ohm with the loss tangent above 0.8.[12, 17, 18] As a result, alternating voltage at this frequency causes homogenous heating. The thermal time constant of the 2 mm diameter plates is below 50 ms [9, 12], allowing the plate to reach thermal equilibrium at any modulation frequency below 20 Hz, as verified with thermal imaging.

We have used the following techniques to monitor electro-thermal actuation:

(1) *Laser Doppler Vibrometer* (LDV) system installed on a wafer prober (Karl Suss SOM4) using the displacement mode of LDV (Polytec GmbH). The LDV is equipped with an OFV-5000 controller and an OFV-534 sensor head. Signals from the LDV were fed into an oscilloscope (Keysight Technologies, DSOX2004A, 70 MHz). The samples were installed on a custom-made holder with built-in heaters for the temperature dependent measurements. External voltage was supplied to the membranes with a waveform generator (Rigol DG4062).

(2) *Atomic force microscope* (AFM, NTEGRA with a SMENA head, NT-MDT Spectral Instruments). Use of the semi-contact mode kept the tip (AC160, Olympus with nominal force constant 40 $N \cdot m^{-1}$) at a fixed distance from the plate top contact. Variations in height were recorded using the z-height sensor, while an alternating voltage was supplied to the plates with the waveform generator (Rigol DG4062). The sample was mounted on a custom-made holder with built-in heaters to test the effect of sample annealing on the room temperature response.

(3) *Michelson-Morley laser interferometer* equipped with a lock-in amplifier (SR830, Stanford Research Systems Inc., USA) was used for the detection of out-of-plane displacements in the middle of the plate. A proportional-integral-derivative (PID) feedback system was built for a working point stabilization against the slow optical path-length drifts. A signal generator Agilent 33210A (Keysight Technologies, USA) was utilized for excitation of the plates.[7, 9, 10, 12]

3 Results

3.1 Electro-thermal effect

Application of an alternating voltage induces Joule heating, as measured with a thermal (IR) camera (CX640, Cox Imaging, **Figure 3**a and **Figure 3**b). The temperature at the center of a membrane can be increased by more than 80K in response to 10 V at 1 MHz (**Figure 3**c). Optical profilometry reveals that the thermally expanded membrane adopts a dome-shape (**Figure 3**d and **Figure 3**e) because the temperature is maximal at the center and decays closer to the edges due to heat conduction to the Si substrate. This is in contrast to the case of homogeneous heating presented in **Figure 2**, which causes the zone at the center of the membrane to remain flat. The out-of-plane deflection at the center reached ≈30 μm (**Figure 3**f) and it could be switched on and off, reversibly, without damaging the membrane. However, four out of five membranes heated electrically to 120 °C in the center did not revert to their initially flat shape, demonstrating some residual deformation.

For the membrane shown in **Figure 3**, the length of the membrane profile between points $X_1$and X_2 on **Figure 3**f (which are distant from each other by $D = X_2 - X_1$ = 1999.8 μm) is L_{ON} = 2002.5 μm with voltage applied and L_{OFF} = 2000.3 μm without voltage. The in-plane strain, with respect to a flat membrane on the onset of buckling, are $u_{ON} = \frac{L_{ON}-D}{D}$ = 1.3×10^{-3} during the "ON" state and $u_{OFF} = \frac{L_{OFF}-D}{D}$ = 2.5×10^{-4} during the "OFF" state. Thus, electro-thermal expansion corresponds to overall linear strain of at least $\Delta u_{xx} > u_{ON} - u_{OFF}$ = 1.1×10^{-3} = 0.11%. It is important to note that the strain is not homogenous throughout the membrane because the temperature change is not homogenous.

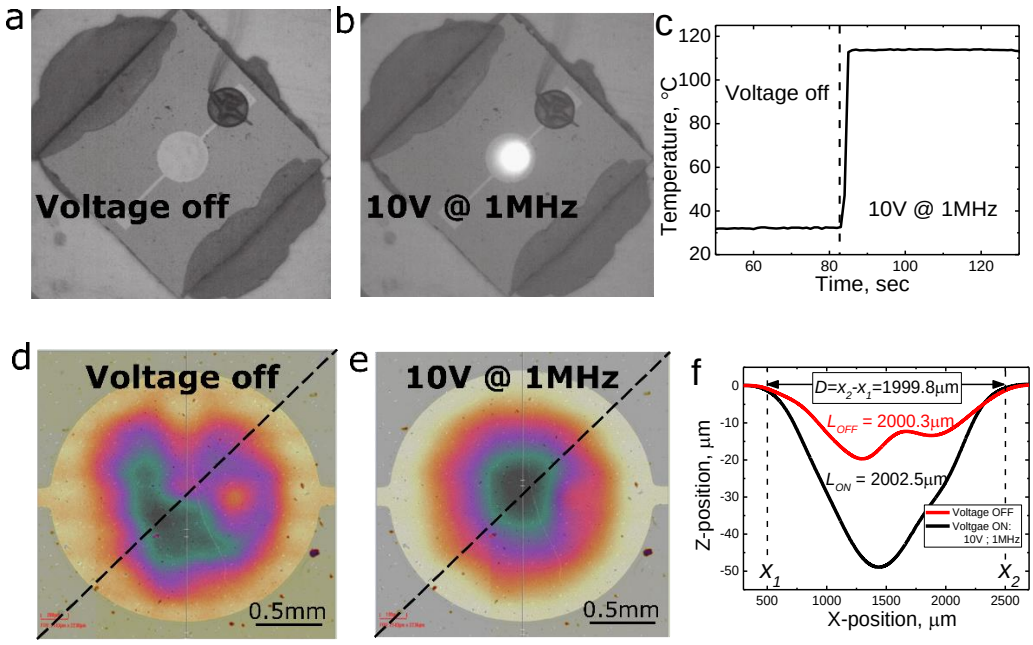

Figure 3. IR image (COX, CX-640 micro) of a self-supported Al/Ag/Ti/CGO5/Ti/Al membrane with (a) no voltage applied and (b) with applied 10 V at 1 MHz. (c) The temperature measured at the center of the membrane in response to applied 10 V at 1 MHz. Optical profiler contour image showing a color map of the membrane out-of-planeprofile; (d) without voltage applied and (e) with applied 10 V at 1 MHz. (f) Scanned profile at the center of the membrane in (d) and (e) showing the change in shape in response to thermal excitation.

3.2 Determination of buckling stress under electro-thermal excitation

As shown in **Figure 4**, the shape of the membrane under electro-thermal excitation, $Z(x,h)$, can be fitted by a Bessel function of the first kind with a 0th integer order (the exact fundamental linear buckling shape of a thin circular plate) according to[16]:

(2) $$Z(x,h) = h \cdot J_0(x \cdot norm),$$

where h is the height at the center, x is the distance from the center of the membrane, and $norm = 2.405$ is the normalization factor for the Bessel function edge at distance 1 mm from the center. The length of the cross-section of a 2 mm diameter membrane is:

(3) $$Length(h) = \int_{-1}^{1} \sqrt{1 + \left(\frac{d}{dx} Z(x,h)\right)^2}\, dx$$

The electro-thermal strain, u_{et}, can, therefore, be determined according to:

(4) $$u_{et} = \frac{Length(h_{final}) - Length(h_{initial})}{Length(h_{initial})}.$$

For the membrane shown in Figure 3, the height at the center under AC heating is h_{ON} = 49 μm (Figure 3f, black curve), which corresponds according to Eq.(4) to u_{et} = 1.4×10^{-3}. This is close to the in-plane strain value measured

directly from the length of the line profile (u_{ON} = 1.3×10^{-3}), with the difference ($u_{ON} < u_{et}$) arising from the fact this specific membrane was not completely flat without voltage applied (Figure 3f, red line).

In order to estimate the stress at the surface of the CGO5 films, one needs to calculate the principal curvature, κ, at the center point of the membrane, which is defined as:

(5) $$\kappa(x,h) = \frac{\left|\frac{d^2}{dx^2}Z(x,h)\right|}{\left[1+\left(\frac{d}{dx}Z(x,h)\right)^2\right]^{3/2}}.$$

Therefore, the maximal bending stress, σ_b, at the surfaces of the CGO5 films, at the center of the membrane (x = 0) can be calculated according to:

(6) $$\sigma_b = \pm Y_b \cdot t_f \cdot \kappa(0,h),$$

where Y_b = 330 GPa is the biaxial unrelaxed Young's modulus of CGO, [19] and t_f = 1.15 μm is the thickness of the CGO5 film.

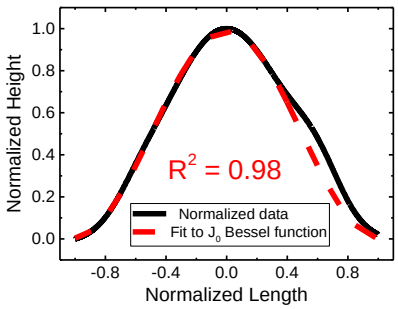

Figure 4. Normalized optical profilometry data (black curve) of the scanned membrane profile (Figure 3f) fitted to a Bessel function of the first kind with 0th integer order (red dashed line).

3.3 Electro-thermal actuation

For a flat membrane, out-of-plane displacement is observed only above a certain threshold voltage (**Figure 5**). This is because before out-of-plane displacement, the voltage-induced thermal expansion should first compensate for the initial in-plane tensile strain in the membrane and the critical buckling strain. Consequently, the out-of-plane displacement signal at 25°C shows a sharp peak shape (**Figure 5**a, black curve). At 55°C, the membrane is already buckled and, therefore, the shape of the response is more sinusoidal (**Figure 5**a, red curve). Moreover, between 25 and 55 °C the response increases and, close to the buckling temperature (50-60 °C), the out-of-plane displacement is a quadratic function of the voltage (**Figure 5**b).

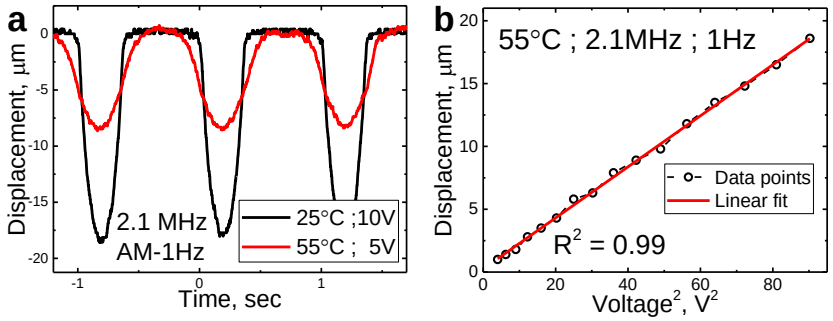

Figure 5. (a) Displacement signal measured with LDV at the center of a self-supported Al/Ag/Ti/CGO5/Ti/Al membrane in response to 10 V at 25°C (black curve) and 5 V at 55°C (red curve) with a carrier frequency 2.1 MHz and an amplitude modulation (AM) frequency of 1 Hz. (b) Displacement as a function the voltage-squared measured at 55°C in response to excitation at 2.1 MHz modulated at 1 Hz. The response fits very well to a linear trend (red line).

3.4 Effect of external heating

After heating above ≈150 °C for more than 20 min, the initially flat membranes (**Figure 6**a) do not restore their flat shape and remain buckled after cooling back to room temperature (**Figure 6**b), indicating that at 150 °C, some of the stress becomes irreversible. We have investigated the response of the membranes to periodic heating with AC voltage before and after annealing at 150 °C using AFM combined with a built-in optical microscope. Before the annealing, periodic heating bends the membrane upwards and no out-of-plane displacement is observed during a large part of the period, when the thermal expansion is insufficient to overcome that tensile strain in the membrane (**Figure 6**c black curve, see also Figure 2 a-c). After the annealing at 150 °C and subsequent buckling, the electro-thermal response was in the opposite direction and the part of the period, at which no out-of-plane displacement occurred was almost gone, indicating that the initial tensile stress was largely relieved (**Figure 6**c, red curve). Since the hardness of doped ceria, including CGO5, exceeds 4 GPa (HV>408) at room temperature [20, 21], it does not exhibit plastic deformation. Therefore, one has to assume that the partial buckling after the annealing is due to relaxation of the stress in the metallic layers.

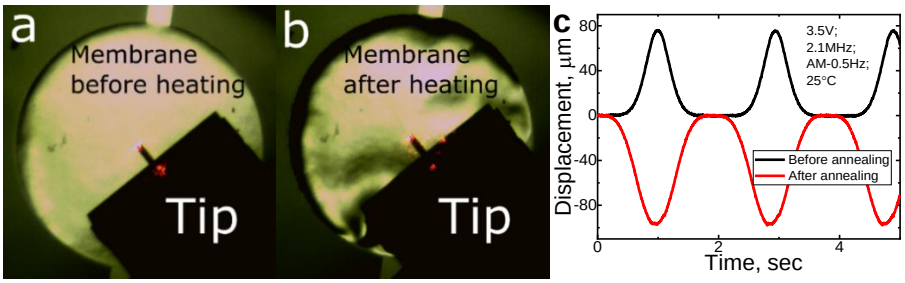

Figure 6. Optical image of a self-supported Al/Ag/Ti/CGO5/Ti/Al membrane in the AFM apparatus (a) before and (b) after heating to 150°C for 20 minutes. (c) The out-of-plane displacement measured at the center of the membrane, using the AFM tip as a probe, before (black curve) and after (red curve) heating.

3.5 Fracture tests

The fracture strength of the membranes was measured with the LDV system by incrementally increasing the excitation voltage to the value at which fracture initiates (**Figure 7**a). Consistently, below the out-of-plane

displacement < 25 μm the surface of the membranes does not show any damage. Catastrophic mechanical failure occurred only with out-of-plane displacement that exceeds 30 μm (**Figure 7**b). For all ten membranes tested, the damage always initiated at the center (**Figure 7**c), where the temperature and, therefore, the curvature are the biggest. Inspection of the damaged membranes with SEM reveals breakage at the CGO columnar grain boundaries (**Figure 7**d) as well as at areas where the CGO detached from the bottom contact (**Figure 7**e).

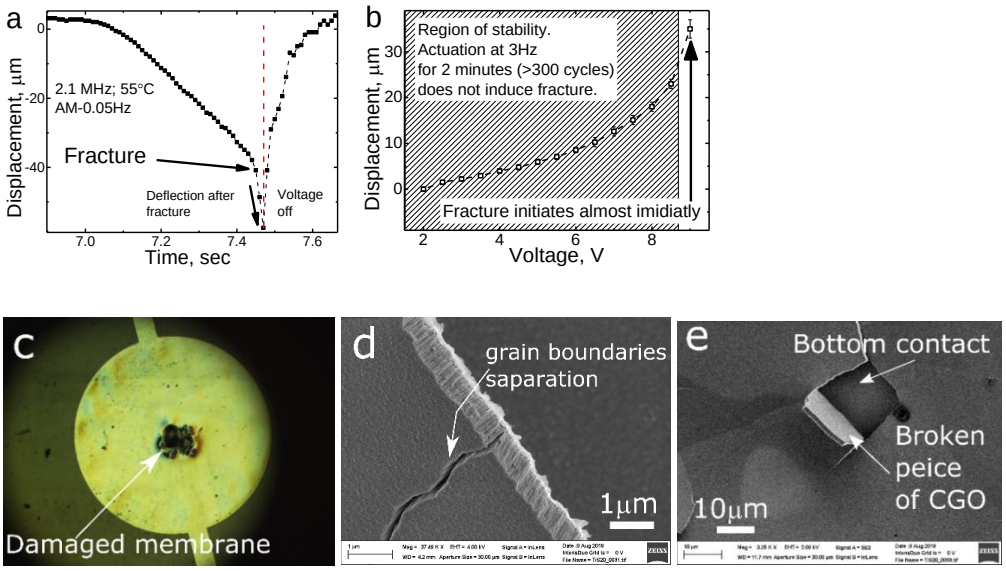

Figure 7. (a) Displacement signal measured at the center of a self-supported Al/Ag/Ti/CGO5/Ti/Al membrane, showing the moment of fracture initiation at 55°C with an excitation of 10 V at 2.1 MHz modulated at 0.05 Hz. Fracture initiated at the first actuation cycle. (b) Displacement vs voltage plot showing two regions of stability: gray region in which actuation persists even after 300 cycles, and a white region in which fracture begin already after a few actuation cycles. (c) Optical image of a damaged membrane showing that failure begins at the center. SEM images of a damaged membrane identifying: (d) region of grain boundary separation, and (e) region where the CGO layer is delaminated from the bottom contact.

The range of the displacement, at which fracture initiated, was between 35 μm and 43 μm and corresponds to the average critical stress of σ_{cr} = 44 ± 4 MPa (**Table 1**). The ultimate tensile stress reported for bulk CGO ceramics is ~150 MPa, [22-24] which is bigger than in the membranes. This is probably because of the columnar orientation of the grains in CGO films, which increases the chance for catastrophic crack propagation.

Table 1. Summary of the displacement amplitude, maximal stress (calculated according to Eq.(6) and conditions at which fracture initiated in the Al/Ag/Ti/CGO5/Ti/Al membranes

Sample number	Displacement at fracture (μm)	Stress (MPa)	Conditions (Voltage, V; frequency, Hz; modulation frequency, Hz; Temperature, °C)
1	35	40.1	10V; 2.1MHz; 1Hz; 80°C
2	38	43.5	9.5V; 2.1MHz; 0.3Hz; 55°C
3	42	48.1	9V; 2.1MHz; 0.05Hz; 55°C
4	43	49.2	10V; 2.1MHz; 1Hz; 55°C
5	36	41.2	9.5V; 2.1MHz; 1Hz; 65°C

3.6 Long term stability at room temperature

To test the stability of the membranes as a function of the number of actuation cycles (fatigue), we monitored the out-of-plane displacement at room temperature during many actuation cycles using the optical interferometer. It was found that out-of-plane displacement of up to 16 μm does not cause any degradation in response below 10^5 cycles @15 Hz (**Figure 8**). A gradual amplitude decline was found to occur above 10^5 cycles, reaching 25% from the original response after 3×10^6 cycles but no signs of mechanical disintegration or cracks were found in the membranes subjected to this test. Moreover, switching the excitation voltage for ≈2 hours was found to recover the original response of the membrane. This strongly suggests that the degradation is related to the charge trapping either at the interface or in the bulk of the membrane, however, because of the very long discharge time (2 hours corresponds to <150 μHz) it was not possible to detect the changes with impedance spectroscopy. During more than a month under thermal actuation, the displacement kept a constant amplitude of 12 µm after 2.6×10^7 cycles. After the long-term fatigue test, the membrane remained flat. It is interesting that a slight increase in the amplitude occurred up to about 10^4 cycles similar to PZT piezoelectric membranes. [25]

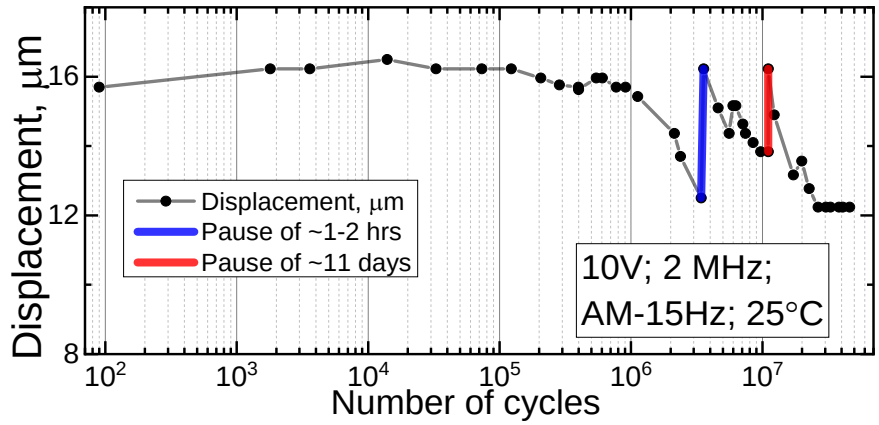

Figure 8. Long-term stability of a flat Al/Ag/Ti/CGO5/Ti/Al membrane measured at room temperature using optical interferometry with excitation voltage of 10 V at 2 MHz with amplitude modulation (AM) of 15Hz. Pauses in the voltage are indicated with blue and red vertical lines.

3.7 Long term stability at elevated temperatures

In order to accelerate fatigue and access larger amplitudes, we have monitored the electro-thermal response at elevated temperatures using the LDV system. For a membrane actuated at 45 °C at 3 Hz with an out-of-plane displacement of ~29 μm (corresponds to $\sim0.7\sigma_{cr}$), the response gradually decreases by ~45% during the course of 250k cycles (**Figure 9**a). The decrease in response follows a logarithmic trend. For a membrane actuated at 65 °C at 10 Hz with initial deflection of 20 μm ($\sim0.5\sigma_{cr}$), the response decreased after 13k cycles by ~40% but then gradually increased (**Figure 9**b) to a constant level of ~14 μm. In all cases, mechanical damage was not observed. All the membranes restored their initially flat shape after cooling back to room temperature.

We also found that the electro-thermal response changes its shape from a sinusoidal one to sharper peak character (red *vs* black curves in **Figure 9**c and **Figure 9**d) during the operation. This suggests that the membranes developed some mechanical tensile strain, the source of which requires further investigation.

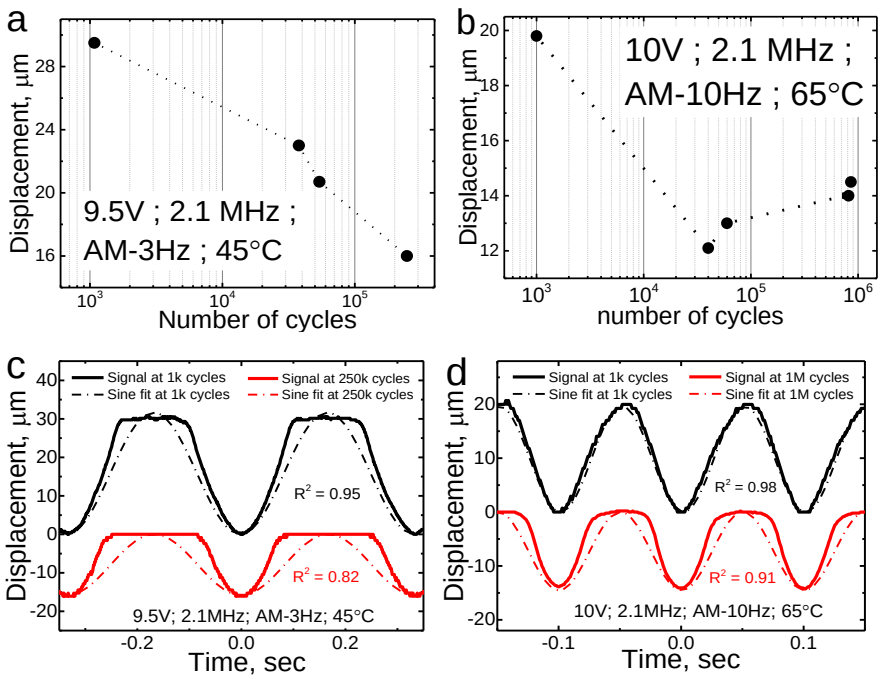

Figure 9. Long-term measurement of the out-of-plane displacement at the center of self-supported Al/Ag/Ti/CGO5/Ti/Al membrane in response to (a) 9.5 V at 2.1 MHz modulated at 3 Hz at 45°C and (b) 10 V at 2.1 MHz modulated at 10 Hz at 65°C. (c) LDV signal for the membrane tested in (a) before (black) and after (red) long-term operation. (d) LDV signal for the membrane tested in (b) before (black) and after (red) long-term operation.

4 Summary

Thermal actuators in the form of self-supported Al/Ag/Ti/CGO5/Ti/Al membranes were used to investigate the stability of CGO as an active material in MEMS actuation devices. The actuator can generate very large deflection (tens of microns) subjected to heating by high frequency (1-2.1 MHz) voltage, enabling determination of fracture strength and long-term endurance to fatigue. With the optically measured deflection, the ultimate strength of the membranes was found to be 44 ± 4 MPa. This is lower than the ultimate tensile stress measured in bulk CGO ceramics, probably because of the columnar grain boundary structure. During long-term operation under periodic loading, it was found that below the critical stress the response gradually decreases. The decrease in response (fatigue) is probably electrical in origin. Damage or mechanical fatigue was not found even after 10^7 actuation cycles at stress levels, which are 35% from the fracture strength of the membranes. The data reported suggests that ceria-based MEMS are viable and can withstand prolonged operation period.

5 Acknowledgement

This work was supported in part by the Israeli Ministry of Science and Technology grant No 3-12421 and #12421-3, the program of Israel-Russian Federation Scientific Collaboration. This work is part of the BioWings project, which has received funding from the European Union's Horizon 2020 under the Future and Emerging Technologies (FET) program with a grant agreement No 801267. This research received funding from the Minerva Center for Self-Repairing Systems for Energy & Sustainability and it is made possible in part by the historic generosity of the Harold Perlman Family. The DRIE unit used for this research was purchased with the Israel Science Foundation Grant # 2366/17.

Part of this work was developed within the scope of the project CICECO-Aveiro Institute of Materials, UIDB/50011/2020 & UIDP/50011/2020, financed by national funds through the FCT/MEC and when appropriate co-financed by FEDER under the PT2020 Partnership Agreement. The equipment of the Ural Center for Shared Use “Modern Nanotechnology” UrFU was used. The research was made possible in part by RFBR (grant 15-52-06006 MNTI_a). The work has been supported in part by the Ministry of Science and Higher Education of the Russian Federation under Project #3.9534.2017/8.9. The work was supported by Government of the Russian Federation (Act 211, Agreement 02.A03.21.0006). S. Krylov acknowledges the support from the Henry and Dinah Krongold Chair of Microelectronics. Y. Shacham-Diamand acknowledges the support from the Bernard L. Schwartz Chair of NanoScale Information Technologies.

6 References

[1] N. Setter, Electroceramic-based MEMS, Springer, 2005.
[2] M.D. Maeder, D. Damjanovic, N. Setter, Lead free piezoelectric materials, J. Electroceram., 13 (2004) 385-392.
[3] H. Inaba, H. Tagawa, Ceria-based solid electrolytes - Review, Sol. State Ionics, 83 (1996) 1-16.
[4] M. Mogensen, N.M. Sammes, G.A. Tompsett, Physical, chemical and electrochemical properties of pure and doped ceria, Sol. State Ionics, 129 (2000) 63-94.
[5] M. Hadad, H. Ashraf, G. Mohanty, C. Sandu, P. Muralt, Key-features in processing and microstructure for achieving giant electrostriction in gadolinium doped ceria thin films, Acta Mater., 118 (2016) 1-7.
[6] R. Korobko, A. Patlolla, A. Kossoy, E. Wachtel, H.L. Tuller, A.I. Frenkel, I. Lubomirsky, Giant Electrostriction in Gd-Doped Ceria, Adv. Mater., 24 (2012) 5857-5861.
[7] E. Mishuk, A. Ushakov, E. Makagon, S.R. Cohen, E. Wachtel, T. Paul, Y. Tsur, V.Y. Shur, A. Kholkin, I. Lubomirsky, Electro-chemomechanical Contribution to Mechanical Actuation in Gd-Doped Ceria Membranes, Adv. Mater. Interfaces, (2019) 1801592.
[8] R. Korobko, A. Lerner, Y. Li, E. Wachtel, A.I. Frenkel, I. Lubomirsky, In-situ extended X-ray absorption fine structure study of electrostriction in Gd doped ceria, Appl. Phys. Lett., 106 (2015) 042904.
[9] E. Mishuk, E. Makagon, E. Wachtel, S. Cohen, R. Popovitz-Biro, I. Lubomirsky, Self-supported Gd-doped ceria films for electromechanical actuation: Fabrication and testing, Sensor Actuat. A-Phys., 264 (2017) 333-340.
[10] N. Yavo, O. Yeheskel, E. Wachtel, D. Ehre, A.I. Frenkel, I. Lubomirsky, Relaxation and saturation of electrostriction in 10 mol% Gd-doped ceria ceramics, Acta Mater., 144 (2018) 411-418.
[11] R. Korobko, E. Wachtel, I. Lubomirsky, Cantilever Resonator Based on the Electrostriction Effect in Gd-Doped Ceria, Sensors and Actuators A, *201* (2013) 73-78.

[12] A. Ushakov, E. Mishuk, D. Alikin, B. Slautin, A. Esin, I. Baturin, V.Y. Shur, I. Lubomirsky, A. Kholkin, in: IOP Conference Series: Materials Science and Engineering, IOP Publishing, 2017, pp. 012008.
[13] M. Varenik, J.C. Nino, E. Wachtel, S. Kim, O. Yeheskel, N. Yavo and I. Lubomirsky, "Dopant concentration controls quasi-static electrostrictive strain response of ceria ceramics" (submitted)
[14] A. Kossoy, Y. Feldman, E. Wachtel, I. Lubomirsky, J. Maier, Elasticity of solids with a large concentration of point defects II. The chemical strain effect in $Ce_{0.8}Gd_{0.2}O_{1.9}$, Adv. Func. Mater., 17 (2007) 2393-2398.
[15] S.P. Timoshenko, J.M. Gere, Theory of Elastic Stability, 2 ed., Dover, NY, 1989.
[16] F. Bloom, D. Coffin, Handbook of Thin Plate Buckling and Postbuckling, CHAPMAN & HALL/CRC, London-New York, 2001.
[17] E. Mishuk, A.D. Ushakov, S.R. Cohen, V.Y. Shur, A.L. Kholkin, I. Lubomirsky, Built-in bias in Gd-doped ceria films and its implication for electromechanical actuation devices, Sol. State Ionics, 327 (2018) 47-51.
[18] E. Mishuk, E. Makagon, E. Wachtel, S.R. Cohen, R. Popovitz-Biro, I. Lubomirsky, Self-supported Gd-doped ceria films for electromechanical actuation: Fabrication and testing, Sensor Actuat A, 264 (2017) 333-340.
[19] N. Yavo, D. Noiman, E. Wachtel, S. Kim, Y. Feldman, I. Lubomirsky, O. Yeheskel, Elastic moduli of pure and gadolinium doped ceria revisited: sound velocity measurements, Scripta Mater., 123 (2016) 86-89.
[20] R. Korobko, S.K. Kim, S. Kim, S.R. Cohen, E. Wachtel, I. Lubomirsky, The Role of Point Defects in the Mechanical Behavior of Doped Ceria Probed by Nanoindentation, Adv. Func. Mater., 23 (2013) 6076-6081.
[21] R. Korobko, C.T. Chen, S. Kim, S.R. Cohen, E. Wachtel, N. Yavo, I. Lubomirsky, Influence of Gd content on the room temperature mechanical properties of Gd-doped ceria, Scripta Mater., 66 (2012) 155-158.
[22] J.-D. Lin, J.-G. Duh, Fracture toughness and hardness of ceria-and yttria-doped tetragonal zirconia ceramics, Mater Chem Phys, 78 (2003) 253-261.
[23] S. Sameshima, T. Ichikawa, M. Kawaminami, Y. Hirata, Thermal and mechanical properties of rare earth-doped ceria ceramics, Mater Chem Phys, 61 (1999) 31-35.
[24] J.E. Shemilt, H.M. Williams, M.J. Edirisinghe, J.R. Evans, B. Ralph, Fracture toughness of doped-ceria ceramics, Scripta Mater., 36 (1997).
[25] A. Kholkin, E. Colla, K. Brooks, P. Muralt, M. Kohli, T. Maeder, D. Taylor, N. Setter, Interferometric study of piezoelectric degradation in ferroelectric thin films, Microelectronic engineering, 29 (1995) 261-264.